

Effect of Post-Flashover Flame Emerging From Opening On External Wall

Wei-Ting Chung* and Kuang-Chung Tsai**

Keywords : external wall fire, building opening, heat flux, flame height, combustion condition.

ABSTRACT

This study performed experiments in which small-scale enclosures with various opening shapes and locations were underpinned for flames on facades emerging from ventilation-controlled fires at the floor of fire origin. To limit uncertainties, a propane gas burner was used to produce controlled heat release rates (30, 40 and 50 kW) as fire source. The size of opening (in W×H) was 20×10 cm², 10×20 cm² and 20×20 cm². Actual heat release rate, gas temperature inside the enclosure, heat flux on the facade wall, and flame contours were measured. Experimental observations and data show that the shape of opening strongly affected the combustion conditions. Opening geometry was divided into two categories: those that combust both inside and outside the enclosure, and combusting primarily outside the enclosure. Two sets of heat flux correlations were derived for the two categories. Additionally, external flame was higher for the category of combustion primarily outside the enclosure, because pyrolyzate primarily burned there. Furthermore, experimental results indicate that the highest heat flux always occurred with the lowest openings, although the difference was not significant.

INTRODUCTION

The initial source of a fire in a building may be outside the practical design constraints. In this case, the fire safety systems may fail, causing external combustion of excess fuel issuing out of an opening as the enclosure fires reach the post flashover state. These external flames tend to attach to the facade of

the building, thus heating it. If the material of the facade is combustible, then the material close to windows on floors above the original fire floor may be ignited, thus spreading the fire from floor to floor. Consequently, facade flames need to be addressed from the behavior of external flames ejecting from enclosure fires. Furthermore, these enclosure fires reach under-ventilated state easily because the enclosure generally has a large fuel load and a small opening. Under-ventilated fires has limited available oxygen flowing through the opening available for burning, leading to incomplete burning of the fuel inside the enclosure, because the mass rate of air inflow is lower than that needed for stoichiometric burning. The unburned fuel then flows out of the opening, and burns outside the enclosure. This external combustion determines the extent of flames outside the enclosure, causing heat exposure to the external wall.

Many studies have investigated the heat exposure to the facade owing to flames emerging from an opening in an enclosure and its dependence on the opening geometry (Delichatsios et al., 2004; Lee et al., 2009; Lee, 2006). Oleszkiewicz (1989) conducted a series of full-scale experiments using a fixed-sized compartment with openings of various geometries to study the magnitude of fire exposure to the exterior wall. Experimental results revealed that the ratio of the window opening height to its width controls the shape of the plume. Additionally, large windows were found to allow more fuel to be burned inside the fire compartment than small windows, thus decreasing the height of the flaming portion of the plume. Bohm and Rasmussen (1987) investigated the relationship of external flame height and radiation on the facade to the rate of heat energy released outside the enclosure. All experiments were conducted under fully developed burning conditions. They (Bohm and Rasmussen, 1987) presented the flame height and incident radiation on the facade above the opening with respect to the heat release rate provided by the external flamer, but did not undertake a detailed analysis. Hasemi (1984) and Yamada et al. (2001) simulated the internal combustible gas outflow through openings by combining a wall and vertical gas burner. The situation is different with actual external fire conditions, because the gas outflow in actual fire conditions is hot

Paper Received September, 2018. Revised March, 2019. Accepted May, 2019. Author for Correspondence: Kuang-Chung Tsai.

* *Ph.D. Student, Department of Safety, Health and Environmental Engineering, National Kaohsiung University of Science and Technology, Taiwan 811, ROC.*

** *Professor, Department of Safety, Health and Environmental Engineering, National Kaohsiung University of Science and Technology, Taiwan 811, ROC.*

and the gas flowing out from the gas burner is cold gas. Yokoi (1960) assumed that the neutral plane is at the half height of the opening, and postulated that the upper half of the opening corresponds to a horizontal rectangular heat source. Accordingly, he proposed a length to represent the outflow of the hot gases at the opening equal to the radius of a circle $r_0 = \sqrt{HW/2\pi}$ having half the area of the opening. Using this length scale, Yokoi (1960) correlated the maximum temperature along the vertical axis. Yokoi's length scale has been extensively employed in correlations of temperature and flame height on external façade. Lee et al. (2012) re-examined Yokoi's length scale, and concluded that Yokoi's correlation is not based on proper dimensional analysis. They subsequently studied the physics of gas ejection from an enclosure, the attachment of flame to the facade wall and the burning of the excess fuel, and observed that the flow development on the facade starts from the convective flow at the exit. Based on this concept, Lee et al. (2012, 2007) proposed two new length scales l_1 and l_2 . l_1 simulates the exit condition of the burning enclosure, assuming that the mass flow rates into the enclosure are equal to that out of the enclosure based on the conservation of mass and taking the burning enclosure as a control volume. l_2 represents the flow behavior in the vicinity of the opening based on the experimental observation: that the flows outside the enclosure are ejected horizontally before turning vertically and attaching to the facade. However, Lee et al. (2012, 2007) applied "door-like" opening for experiments, and the effects of "window-like" opening locations and on the heat exposure to the external facade are not incorporated into current engineering fire design methods. To clarify this issue, the present study investigates the temperature distribution inside the enclosure, the flame height and the heat flux to the external wall by undertaking experiments on a reduced scale experimental model with various opening locations (window and door), opening geometry and fire supply rate. Finally, the experimental data for window-like openings are incorporated into the current correlations for door-like openings.

EXPERIMENTAL SET-UP AND PROCEDURE

Figure 1 shows the detailed experimental configuration. The experimental enclosure is a cube with the size of $0.5 \times 0.5 \times 0.5 \text{ m}^3$ and built of ceramic fiberboard. Table 1 presents the size ($20 \times 10 \text{ cm}^2$, $10 \times 20 \text{ cm}^2$ and $20 \times 20 \text{ cm}^2$ in $W \times H$) and location (up, middle and down) of the opening, which was designed at the front face. Propane from a rectangular sandbox burner was the fuel source to precisely regulate the fuel supply rate (30 kW, 40 kW and 50 kW, nominally) by a mass flow controller. The burner was located at

the center of the floor. The external facade was formed of a fiberboard plate with steel plate heat flux gauges with intervals of 10 cm installed on the central line. This apparatus consists of a steel plate with a thermocouple extension line spot-welded to the rear surface of the plate. The steel plate gauge with dimensions 25 mm by 25 mm by 3 mm was employed in this work to measure heat fluxes in the facade wall. This design is consistent with that used by Lee et al. (2009). Additionally, two thermocouple trees with interval of 10 cm were placed in an outer and an inner corner. The whole rig was located under a calorimeter hood to measure the heat release rate according to the oxygen consumption principle (Janssens, 1991).

The experimental procedure was designed to establish steady state conditions inside the enclosure. At the beginning of each test, the flow rate of the fuel was increased at a fixed rate (50 mg/s) every 30 seconds after its ignition until the required (or theoretical) flow was reached (30 kW in 270 seconds, 40 kW in 420 seconds and 50 kW in 540 seconds). A horizontal fiberboard plate was placed over the opening to deflect the flames, and thus prevent the flame from impinging on the facade and imposing a heat flux on the steel plate gauges during this period. The horizontal fiberboard was then removed after steady conditions were established. The flames were then attached to the facade, and exposed to the heat flux gauges. The appearance of the ejecting flame was recorded by a CCD camera facing the façade, enabling the measurement of the ejecting flame height. Subsequently, the gas temperatures inside the enclosure, actual heat release rate and total heat flux at different locations in the façade were measured by the apparatus described above. Each case was conducted three times. Adequate consistency was demonstrated.

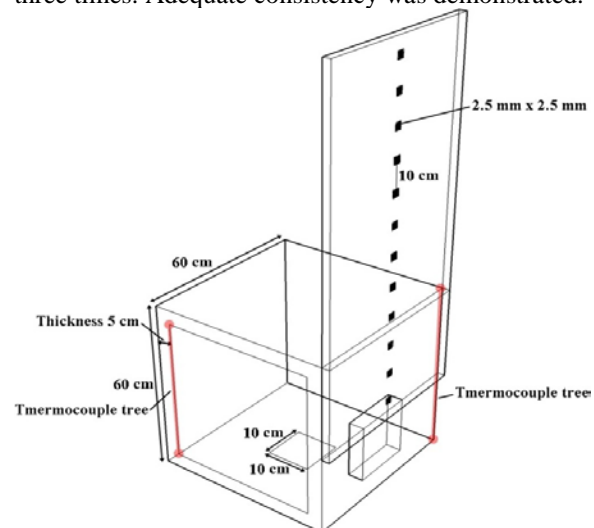


Fig. 1. Geometry of the enclosure and the facade with its instrumentations.

Table 1. Opening conditions and internal HRR

Opening Geometry	Opening size W×H (m)	HRR (kW)	Theoretical 1500AH ^{1/2} (kW)	Estimated internal HRR after flashover (kW)		
				Opening Location		
				Down	Mid	Up
	0.2×0.2	40	26.83			
		50		17.55±1.54	16.96±1.88	19.40±2.51
	0.1×0.2	30	13.42	9.33±2.03	10.16±1.44	10.41±3.45
		40		10.45±1.47	11.17±2.34	11.36±2.48
	0.2×0.1	50	9.49	10.97±1.51	11.49±2.54	11.65±3.59
		30		~0	~0	~0
		40		~0	~0	~0
		50		~0	~0	~0

EXPERIMENTAL RESULTS AND DISCUSSION

The experiments were designed to produce ventilation controlled fires by controlling the mass flow rate of the fuel larger than the fuel needed for stoichiometric combustion with the air entering into the enclosure.

Figure 2 illustrates the temperature histories inside the burning enclosure of the 50 kW fires with different opening geometries. The opening was in the “down” position. Clearly, the temperature rose with time, and started to diverge at approximately 200 s. The temperature continued to increase for the fires with the 20×20 cm² and 10×20 cm² openings, but started to decline for the fire with the 20×10 cm² opening. Therefore, the fires were fuel-controlled in all cases before 200 s, and the fuel was combusted primarily inside the enclosure. Further, Figure 3 depicts the experimental observations of flames emerging out of the enclosure for those tests during steady state (at approximately 400 s). Observation results show that the combustion conditions can be divided into two categories according to opening geometrics: combustion primarily outside the enclosure (20×10 cm²) and combustion both inside and outside the enclosure (20 ×20 cm², 10×20 cm²). Observations were consistent for all openings cases. The flame emerging from the 20×10 cm² opening covered it, preventing air from easily entering the enclosure, thereby causing inactive burning inside the enclosure. Consequently, most of the excess pyrolyzate issued out of the enclosure, and burned outside forming a fire plume on the external facade wall.

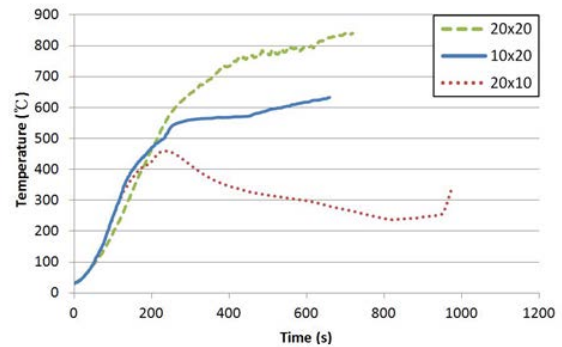


Fig. 2. Temperature histories inside the burning enclosure of the 50 kW fires with different opening geometries at “down” position.

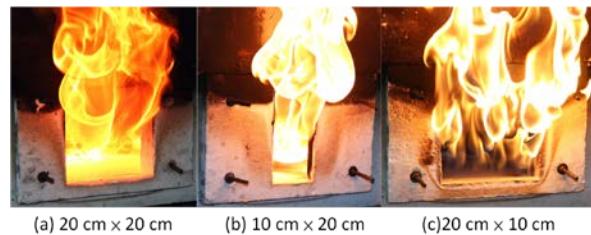


Fig. 3. The flames emerging from the enclosure with different opening shape.

Actual heat release rate

This experimental study examined the effect of opening area and location on the HRR. Figure 4 displays the actual heat release rate measured for the nominal 50 kW fires with middle opening. The measured HRR was highest with the 20×20 cm² opening, and lowest with the 20×10 cm² opening. The reason for this may be the fuel having a lower temperature before burning with the 20×10 cm² opening because the fuel was burned outside the enclosure without preheating. The fuel with the 20×20 cm² and 10×20 cm² openings was heated by the fire

inside the enclosure and was hot when it emitted from the openings. Hotter fuel led to greater combustion completeness. Consistent results were observed for all openings cases. Moreover, Figure 5 displays the measured total HRR for nominal 50 kW fires with 20×20 cm² opening at different positions (up, middle or down). The HRR histories were almost identical. Therefore, the opening area and shape have little effect on HRR, but the opening position (window or door) has no effect.

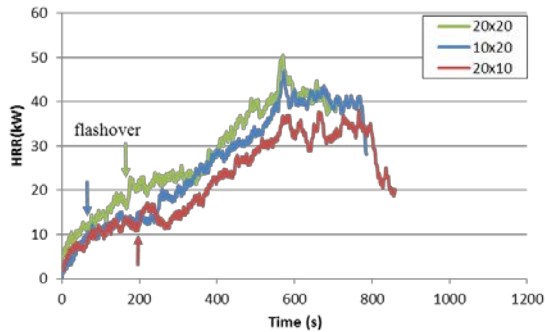


Fig. 4. Heat release rate history for three openings geometrics of middle opening location. The nominal HRR is 50 kW.

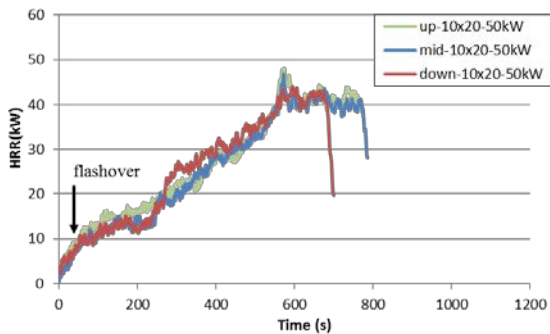


Fig. 5. The measured total HRR for nominal 50 kW fires with the 10×20 cm² opening at different positions (up, middle or down).

HRR inside and outside the enclosure

As described above, the combustion conditions in this experiment can be divided into two categories according to opening geometrics: combustion primarily outside the enclosure (20×10 cm²) and combustion both inside and outside the enclosure (20×20 cm², 10×20 cm²). The heat appears to be produced inside and outside the enclosure.

$$\dot{Q}_{tot} = \dot{Q}_{int} + \dot{Q}_{ext} \quad (1)$$

where \dot{Q}_{tot} is the total HRR
 \dot{Q}_{int} is the internal HRR
 \dot{Q}_{ext} denotes the external HRR

Kawagoe (1967) investigated the theoretical HRR after flashover inside the enclosure, given $1500A\sqrt{H}$, while Drysdale (2011) found that $750A\sqrt{H}$ was a more practical value. Lee et al. (2007) used this value of $1500A\sqrt{H}$ to represent the \dot{Q}_{int} since they found that an intermediate plateau value in HRR history was equal to $1500 A\sqrt{H}$. However, this intermediate plateau value in HRR histories was not seen in all tests although was observed in some “down” opening tests (see Fig. 4 and 5). This study experimentally estimated the HRR inside the enclosure after flashover to be the HRR at 30 s before flashover from the HRR histories for each test. Table 1 lists the theoretical values, $1500A\sqrt{H}$, and estimated internal HRR after flashover. Generally, the \dot{Q}_{int} was higher for higher openings. For the cases with the 20×10 cm² opening, the \dot{Q}_{int} was estimated to be close to 0 kW because no flame was observed inside the enclosure.

Steady state gas temperatures inside the enclosure

Figure 6 shows the steady state gas temperature distributions inside the enclosure for all experiments. The remarks from this figure are:

- (a) When the opening geometrics were 20×20 cm² and 10×20 cm², the temperatures inside the enclosure were approximately 800°C and 600 °C , respectively. Clearly, more air can be entrained into the enclosure for burning when the opening is larger, thus increasing the temperature. This observation was consistent with that of Oleszkiewicz (1989), and confirmed that the fires were ventilation-controlled. Additionally, the steady state gas temperatures inside the enclosure did not depend on the supplied theoretical heat release rate for the same opening and the same opening locations. Furthermore, the steady state gas temperature distribution inside the enclosure was quite uniform from the top to the floor of the enclosure, except in the very low space (i.e. below 10 cm) where air can be entrained and mixed with fuel.
- (b) The temperatures inside the enclosure when the opening was 20×10 cm² were 200-420°C . Most fuel burned outside the enclosure. Moreover, the temperatures inside the enclosure were higher for fuels with lower nominal HRR and with upper opening location. The combustion completeness was higher when less fuel was generated in the enclosure with the 20×10 cm² opening, because the air entrained from outside was limited. Additionally, more fuel can issue out of the enclosure with higher opening, while more fuel can accumulate inside the enclosure with lower opening, thus increasing the concentration of pyrolyzate. Pyrolyzate with higher concentration released more heat.

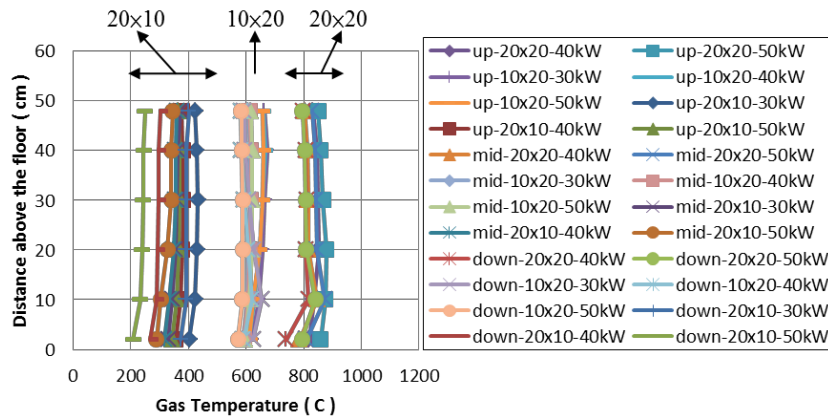


Fig. 6. Vertical temperature distribution measured by the front thermocouple tree for all experiment data.

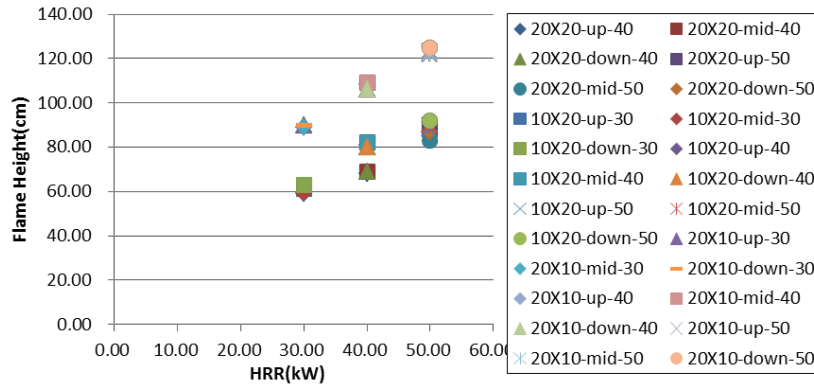


Fig. 7. Comparison of flame height for different openings geometrics and locations with different fuel supply rates.

Flame heights

The flame height and the flame width outside the enclosure were recorded by a CCD camera facing the facade. The flame heights were determined from the location of the neutral plane of the opening, which in this study was located at approximate 0.4 H from the bottom of the opening for ventilation controlled conditions. Figure 7 shows the flame height data for propane plotted against the nominal heat release rate from the burner. The external flame heights increased only with fuel supply rate, and were independent of the opening location. Additionally, the flame height was highest when the opening geometrics was 20×10 cm². The fuel consumption was very low inside, but much higher outside to generate high flames. Therefore, flame spread to an upper floor may most likely occur with the opening geometrics of 20×10 cm².

Figure. 8 shows the correlation of the flame height based on the actual external HRR and the length scale ℓ_2 (Lee et al., 2007).

$$\frac{Z_f}{\ell_2} = \text{fcn}(\dot{Q}_{\ell_2}^*) = \text{fcn} \left[\frac{\dot{Q}_{\text{ext}}}{\rho_{\infty} c_p T_{\infty} \sqrt{g} \ell_2^{5/2}} \right], \quad (2)$$

where $\ell_2 = (AH^2)^{\frac{1}{4}}$. (Lee et al., 2012, 2007)

It can be observed that the flame height Z_f/ℓ_2 correlates well with $\dot{Q}_{\ell_2}^*$, giving

$$\frac{Z_f}{\ell_2} = 3.81 \dot{Q}_{\ell_2}^{*0.52}. \quad (3)$$

The correlation derived in this study is close to that from Lee et al. (2007). Additionally, the power dependence of flame height on the heat release rate was 1/2, between 2/5 and 2/3, i.e. characteristic power values for two-dimensional and three-dimensional fires, respectively (Lee et al., 2007).

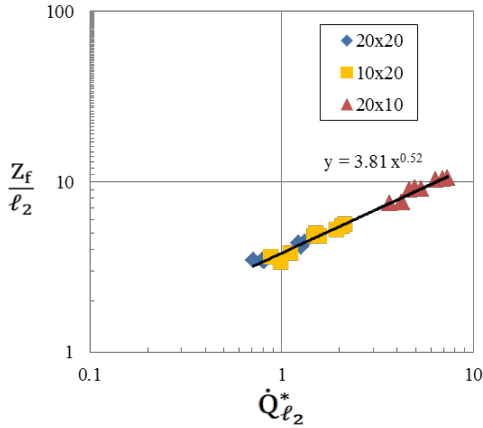


Fig. 8. Flame height correlation for all experiments.

Heat fluxes

According to the previous section, the combustion conditions are divided into two categories, combustion both inside and outside the enclosure, i.e. 20×20 cm² and 10×20 cm², combustion primarily outside the enclosure, i.e. 20×10 cm². Figure 9 shows the heat flux distributions along the centerline above the opening against Z/Z_f for experiments with 50 kW HRR, 20×10 cm²/20×20 cm² opening and various opening locations, where Z and Z_f denote the location on the external facade of the heat flux gauge and the measured flame height, respectively. Clearly, higher heat flux always occurred with lower opening. This finding may be caused by preheating of fuel pyrolyzate for which can be accumulated by lintel barrier for certain period before burning. Additionally, the heat flux was higher with the 20×10 cm² opening than the other openings. The higher heat flux was primarily due to the flame inclined to the façade much more obvious for the tests having opening with wide width and shallow depth shape compared with those openings having narrow width and higher depth shape. Additionally, the flame from the 20×10 cm² opening

was thinner. The closer distance between the flame and the façade caused more radiation to the façade although the flame was thinner.

The measured heat fluxes at the centerline of the facade wall were correlated based on dimensional analysis from Lee et al. (2007).

$$\frac{q''_t Z_f e^{0.6(H/\ell_2)}}{Q_{ext}/\ell_2} = \text{function} \left(\frac{Z}{Z_f} \right) . \tag{4}$$

Figure 10 plots the data for all tests. Two lines can be identified: the upper line corresponds to the combustion both inside and outside the enclosure and the lower line corresponds to combustion primarily outside the enclosure, respectively. For the category of combustion both inside and outside the enclosure, the heat flux on the façade from window-like openings was close to that from door-like openings (Lee et al., 2007), given Equations (5) and (6).

$$\frac{q''_t Z_f e^{0.6(H/\ell_2)}}{Q_{ext}/\ell_2} = 0.23 \quad \text{for } \frac{Z}{Z_f} \leq 0.35 , \tag{5}$$

$$\frac{q''_t Z_f e^{0.6(H/\ell_2)}}{Q_{ext}/\ell_2} = 0.073 \left(\frac{Z}{Z_f} \right)^{-1.6} \quad \text{for } \frac{Z}{Z_f} > 0.35 . \tag{6}$$

Equations (7) and (8) were provided for the category of combustion outside the enclosure.

$$\frac{q''_t Z_f e^{0.6(H/\ell_2)}}{Q_{ext}/\ell_2} = 0.12 \quad \text{for } \frac{Z}{Z_f} \leq 0.35 , \tag{7}$$

$$\frac{q''_t Z_f e^{0.6(H/\ell_2)}}{Q_{ext}/\ell_2} = 0.049 \left(\frac{Z}{Z_f} \right)^{-1.6} \quad \text{for } \frac{Z}{Z_f} > 0.35 . \tag{8}$$

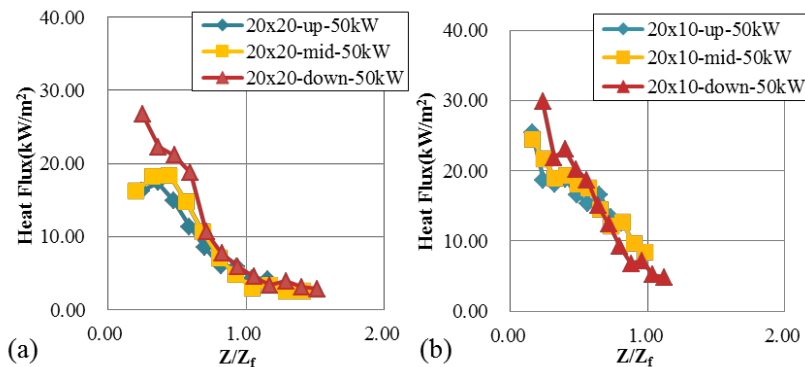


Fig. 9. (a) Heat flux distribution along the centerline above the opening for the combustion both inside and outside the enclosure. (b) Heat flux distribution along the centerline above the opening for the combustion primarily outside the enclosure.

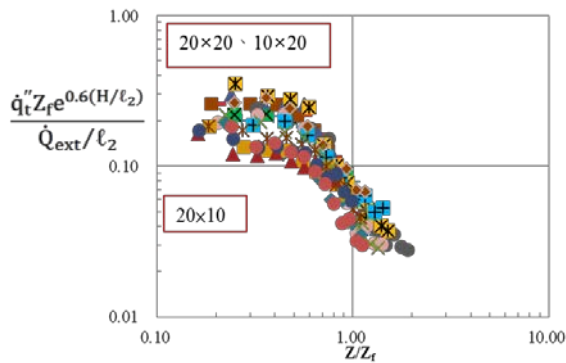


Fig. 10. Heat flux correlation at the centerline of the facade for all tests.

CONCLUSIONS

This study provided correlations for flames on facades as the flames emerge from flashover fires in enclosure. Namely, the main contributions are:

- (1) The combustion conditions of an enclosure fire can be divided into two categories: combustion primarily outside the enclosure and combustion both inside and outside the enclosure. The combustion condition is linked to the size and shape of opening.
- (2) The combustion condition significantly influences the external flame height. The flame height is highest when opening geometry is 20×10 cm². Therefore, the flame is most likely to spread to an upper floor occur with the opening geometry of 20×10 cm². Additionally, the external flame height increases only with the fuel supply rate for identical opening geometry, and is independent of the opening location.
- (3) A higher heat flux on the façade wall always occurs with lower opening because the fuel pyrolyzate is accumulated by lintel barrier for certain period before burning, and is preheated.
- (4) The heat flux was higher with the 20×10 cm² opening than the other openings because more fuel pyrolyzate burns outside from the 20×10 cm² opening. A thicker external flame is formed, causing more radiation to the façade.
- (5) The correlation from Lee et al. (2007) can adequately correlate the data of window opening when the combustion condition is categorized both outside and inside the enclosure. Another series of correlations is provided when the combustion condition is categorized primarily outside the enclosure.

REFERENCES

Bohm, B. and Rasmussen, B.M., "The Development of a Small-scale Fire Compartment in Order to Determine Thermal Exposure Inside and Outside Buildings," *Fire Saf. J.*, Vol. 12, pp.

103-108 (1987).

Drysdale, D., *An Introduction to Fire Dynamics*, John Wiley & Son Ltd. (2011)

Delichatsios, M.A., Silcock, G.W.H., Liu, X., Delichatsios, M. and Lee, Y.P., "Mass Pyrolysis rates and Excess Pyrolyzate in Fully Developed Enclosure Fires," *Fire Saf. J.*, Vol. 39, pp. 1-24 (2004).

Hasemi, Y., "Experimental Wall Flame Heat Transfer Correlations For The Analysis of Upward Wall Flame Spread," *Fire Sci. Technol.*, Vol.4, pp. 75-90 (1984).

Janssens, M.L., "Measuring rate of heat release by oxygen consumption," *Fire Technol.*, Vol. 27, pp. 234-249 (1991).

Kawagoe, K. and Sekine, T., "Estimation of Fire Temperature-Time curve in Rooms," Building Research Institute Report 29, Japanese Ministry of Construction (1967).

Lee, Y.P., Delichatsios, M.A. and Ohmiya, Y., "The Physics of the Outflow from the Opening of an Enclosure Fire and Re-examination of Yokoi's Correlation," *Fire Saf. J.*, Vol. 49, pp. 82-88 (2012).

Lee, Y.P., Delichatsios, M.A., Ohmiya, Y., Wakatsuki, K., Yanagisawa, A. and Goto, D., "Heat Fluxes on Opposite Building Wall by Flames Emerging from an Enclosure," *Proc. Combust. Inst.*, Vol. 32, pp. 2551-2558 (2009).

Lee, Y.P., Delichatsios, M.A. and Silcock, G.W.H., "Heat Fluxes and Flame Heights in Facades from Fires in Enclosures of Varying Geometry," *Proc. Combust. Inst.*, Vol. 31, pp. 2521-2528 (2007).

Lee, Y.P., "Heat Fluxes and Flame Heights in External Facade Fires," Ph.D. thesis, University of Ulster, FireSERT (2006).

Oleszkiewicz, I., "Heat Transfer from a Window Fire Plume to a Building Facade," *Collected papers in Heat Transfer*, Vol. 123, pp. 163-70 (1989).

Yamada, T., Takanashi, K., Suzuki, T., Yanai, E., Sekizawa, A., Satoh, H. and Kurioka, H., "An Experimental Study of Ejected Flames' Configuration by Processing VCR Pictures," *Proceeding, 5th AOSFST*, Newcastle, Australia, pp. 476-478 (2001).

Yokoi, S., "Trajectory of Hot Gas Ejected from a Window of a Burning Concrete Building", *Building Research Institute Report 34*, Japanese Ministry of Construction, pp. 78-89 (1960).

居室火災閃燃後火焰竄出 開口對外牆影響之研究

鐘偉庭 蔡匡忠

國立高雄科技大學環境與安全衛生工程系

摘要

當侷限空間內可燃物引燃之後，火焰快速蔓延擴大而引發閃燃現象，將引發外部燃燒現象進而造成火勢向建築物上層延燒之情形發生。因此，本研究設計三種開口模式（上、中、下）、三種不同的開口形狀（20cm×20cm、20cm×10cm、10cm×20cm）以及三種熱釋放率（30 kW、40 kW、50 kW），並進行一系列的縮小尺寸實驗，探討不同開口形狀與開口模式，對室內燃燒之影響，亦探討於不同變因條件下，火焰竄出開口後對外牆造成之影響與觀察外部火焰形狀的變化。研究結果發現，燃燒情形可依開口形狀分成主要在室外燃燒（20cm×10cm）與室內外皆有燃燒（20cm×20cm 及 10cm×20cm）兩大類。觀察外部燃燒情形發現，其火焰高度並不會隨開口位置的改變而變化，熱通量計量測部分顯示，當開口位置位於下方時，外部火焰對牆面造成的熱通量最大，其原因為氣體燃燒器所噴出之低溫可燃氣體因被門楣阻擋而累積於室內加溫，並轉為高溫可燃氣體後才流出室外，造成竄出開口之火焰溫度高於其它開口位置，進而提高對外牆造成之熱通量。